Click here to view PowerPoint presentation; Press Esc to exit

Advanced Sensor Components for Space-Based Surveillance and Situational Awareness

T. Apostolova, D.A. Cardimona, D.H. Huang, D.T. Le,
P.M. Alsing, W. Glass and C.D. Castillo
Air Force Research Laboratory, Space Vehicles Directorate
3550 Aberdeen Ave., S.E.
Kirtland AFB, NM 87117-5776

ABSTRACT

The ability to reconfigure a sensor in order to enhance performance or perform multiple missions is a very desirable attribute for future sensor systems. If a sensor could reconfigure itself to exploit signals at various wavelengths from the UV through the IR and into the millimeter-wave regimes, that system could support situational awareness missions such as cold-body detection, target discrimination and identification, target status determination, etc., or surveillance missions such as plume-to-hard-body handover, surveillance through clouds, chemical/biological weapons detection, etc., and would be assured of operation 24 hours/day, 7 days/week, in all weather conditions and at very long distances. If this reconfiguration could be done with a single detector, the savings in cost, weight, and power consumption would be substantial. In this paper we present some ideas for tuning the wavelength response of detectors throughout the IR, and possibly into the terahertz (using applied electric or magnetic fields). We also present a device concept for detecting the full polarization vector of a signal within a single pixel of a quantum well detector. Finally, we describe a concept for cooling the detector directly on the chip, pixel by pixel, thereby reducing the volume, weight, and resulting cost of the entire sensor.

1. INTRODUCTION

Infrared sensors are key elements of surveillance and reconnaissance systems. Tactical surveillance and reconnaissance missions usually require Infrared (IR) Focal Plane Arrays (FPAs) operating in atmospheric "windows" where IR transmission is high. The vast majority of applications are in the Long-Wave Infrared (LWIR) window (8-14μm) with a small number of applications in the Mid-Wave Infrared (MWIR) (3-5μm) window. On the other hand, space surveillance of space (such as in space situational awareness) requires observation of extremely faint targets against dark backgrounds. These missions call for LWIR or Very-Long-Wave Infrared (VLWIR) FPAs (14 - 28μm) to detect cold objects and/or to help discriminate between reentry vehicles, decoys, balloons and lightweight replicas with less thermal mass, solar glint off small debris, and hot combustion products. For these types of missions, multiple wavelength arrays can effectively measure the thermal characteristics of these targets using the ratio of MWIR and LWIR measurements. For advanced threats, colder targets (below 300K) or thermally-shrouded targets may be encountered and at least one detector waveband must extend into the VLWIR region for effective thermal measurements. In addition, many of these objects emit in the millimeter-wave (mm-wave or THz) region of the spectrum, as do many biological and chemical agents. The ability to detect these extremely long wavelengths will certainly enhance the detection and identification of such materials. Of course, it is always interesting to look at targets in the visible, as well. Finally, the ability to see in the ultraviolet (UV) will enable solar-blind missions, and

Apostolova, T.; Cardimona, D.A.; Huang, D.H.; Le, D.T.; Alsing, P.M.; Glass, W.; Castillo, C.D. (2005) Advanced Sensor Components for Space-Based Surveillance and Situational Awareness. In *Emerging EO Phenomenology* (pp. 1-1 – 1-14). Meeting Proceedings RTO-MP-SET-094, Paper 1. Neuilly-sur-Seine, France: RTO. Available from: http://www.rto.nato.int/abstracts.asp.

comparing UV and visible spectra will enable materials identification. Now, if any or all of those wavelength ranges could be detected within a single detector, we would have an extremely responsive low-cost sensor system that could be reconfigured for whatever mission we desire.

The field of nanoscience includes the study of synthetic nanostructures created by nanometer-scale building blocks. What makes synthetic nanostructures so attractive is that electrons no longer flow through conductors like rivers. On this scale, the wave nature of an electron is observable, such as an electron tunneling through a thin insulating layer or the self-selection of the polarization of an optical response. These features can often be exploited for creating electronic and electro-optic devices and components. A multiple-quantum-well (MQW) structure is one example of a synthetic nanostructure built by sandwiching a 5 - 10 nanometer (nm) layer of a narrower bandgap semiconductor material (e.g., GaAs) between layers of a similar material with a wider bandgap (e.g., AlGaAs) (thus forming a "well" surrounded by "barriers" in energy-position space) in a repeated pattern. The sharp interface between the well and barrier materials and the nanometer scale of the well thickness provide a strong confinement to electrons in the direction perpendicular to the well layers. As a result, electron motion in the direction of confinement becomes quantized and subband energy levels are formed. The number of confined energy levels and their separation depend on the well and barrier material and dimensions. In principle, the energy separation can be tailored to respond to incident light with wavelengths ranging from MWIR to VLWIR, and under special conditions even longer (to mm-wave).

Quantum well infrared photodetectors (QWIPs), which employ the unique optical and transport characteristics of MQWs, are based on intersubband absorption in III-V semiconductor multiple quantum well heterostructures, and have been rapidly developed to the point where they are now extremely attractive for a growing number of sensor applications. These detectors lend themselves exceptionally well to bandgap engineering of the wavelength response. QWIPs exhibit very high uniformity and their fabrication is relatively cheap when compared with mercury-cadmium-telluride and silicon-IBC detectors. QWIPs can be engineered for any cutoff wavelength of interest between 4 and 25 microns. Also, large format QWIP arrays are easily attainable (640 x 480 has been demonstrated in a camera, and 4096 x 4096 has been fabricated). These devices can be tailor-made to detect long wavelength IR radiation (20μm or longer), and they present the exciting possibility of multi-wavelength detection within a single pixel. MWIR/MWIR, MWIR/LWIR and LWIR/VLWIR QWIP arrays have been demonstrated. Due to the quantum confinement of the electrons within QWIPs, they also have the unique capability that their peak wavelength response can be tuned with an applied bias voltage or an applied magnetic field.

2. LATERAL BIASING FOR TUNING THE DETECTED WAVELENGTH

One sensor feature that enables object discrimination and identification is the ability to determine the exact spectral signature of the object. Currently, this feature is implemented using spectral filters and multiple FPAs, each with its own set of optical elements. Bandgap-engineered QWIPs, as well as quantum dot infrared photodetectors (QDIPs) have been shown to exhibit a voltage-tuning capability where the spectral response of a single device can be "tuned" when a bias voltage applied across the growth layers (parallel to the growth direction) is varied. This voltage tuning is produced by the quantum-confined Stark Effect – the shifting of quantized energy levels due to an applied electric field. Voltage tunability can be used to determine the exact spectral signature of the target, without the use of spectral filters or multiple FPA channels. This could result in a significant reduction in the complexity, cost, and weight of the sensor.

The above so-called vertical biasing is not the only possibility. We can also apply a bias field laterally across the pixel, parallel to the plane of the quantum wells (perpendicular to the growth direction). In this case, we first design an asymmetric double quantum well (DQW) structure with a thin middle barrier between the two wells. In this asymmetric DQW structure, a narrow well doped with electrons contains a ground state and an excited state, while a step-lifted wide undoped well contains only one state, resonant with the excited state in the narrow well (see Fig. 1). The most important innovation of this DQW structure is that the two quantum wells can be independently biased laterally from the sides of the pixel, so that planar transport instead of vertical transport can occur in the individual wells and can be controlled independently. The step up to the wide well will be used to reduce the dark current when it is biased laterally. When the electrons in the narrow quantum well absorb a photon, they can transit to the upper excited state in the same well and then rapidly move into the wide well through a resonant tunneling process due to the thin barrier between these two wells. Consequently, the electrons in the wide well will be swept to the collector region when the lateral bias is applied to this well. Because the photo-excited electrons are driven by the lateral bias in one of the quantum wells, a unit optical gain is expected due to the lack of carrier capture processes in the transport (compared to 20% or less in vertically-biased QWIPs). In addition, the bias voltage required can be very low compared to that in normal QWIPs.

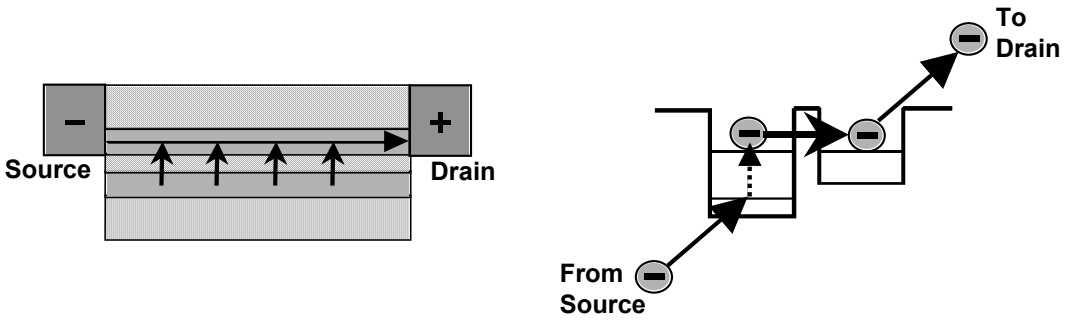

Figure 1: Laterally-biased double quantum well system. On the left we see the conduction path from the source (-) to the drain (+). Electrons in the bottom well absorb a photon and then tunnel through the narrow barrier to the other well, where they feel the bias field and are swept out of the detector and collected as photocurrent. On the right is the band structure diagram for this process.

The requirement of independent control of the lateral bias within each well can be eliminated if we include gate biases to control the current flow within each quantum well due to a common lateral bias. (see Fig. 2) In this case, the upper and lower gate voltages deplete the regions shown in the figure, thus forcing current to flow as shown. By varying either the lateral bias, or the vertical gate bias, the wavelength responsivity can be tuned continuously from the LWIR to the VLWIR and beyond.

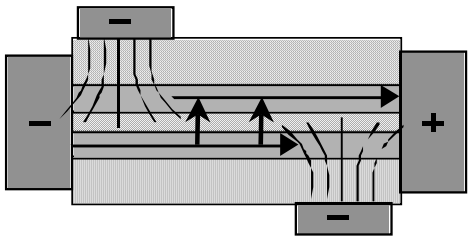

Figure 2: The lateral conduction path when top and bottom gates are biased.

3. QUANTUM DOT DETECTORS

A very important issue that needs to be addressed in GaAs/AlGaAs QWIPs is their relatively low optical coupling efficiency due to an inability to detect normally-incident radiation without a grating (there must be a component of the incident electric field in the confinement direction, i.e., the growth direction). If we could confine the electrons in all three dimensions, these electrons would not be restricted in their coupling to an electromagnetic field. Confinement in three dimensions is called a quantum dot (QD) (of course, atoms are also 3D-confined objects; however, we will restrict our discussion to laboratory-engineered semiconductor structures). The QDs we studied were all fabricated in the Stanski-Krastnov growth mode.[1] Growth of highly mismatched semiconductors leads to the spontaneous formation of islands. The nucleation of the pseudomorphic islands is driven by the strain, and results in the formation of self-organized QDs. Dot formation or coherent islanding occurs to relieve the strain of the lattice mismatch. As the AFM image in Fig. 3 shows, the dots formed with InAs on GaAs are more like pyramids. Their base lengths range from 10 – 20 nm with a height of 2-3 nm.

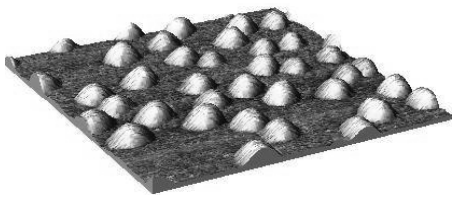

Figure 3: AFM image of single layer of quantum dots (image taken at the Center for High Technology Materials, University of New Mexico).

Depending on the growth conditions, different shapes, either pyramidal or lens-like, can be obtained for the islands. Of considerable importance is the fact that the dots are grown epitaxially. Dot densities in the range of $>5x10^{10}$ cm^{-2} are common. Since absorption of the signal photons will occur within these QDs, this density is not very large. To increase the absorption cross section, the dots can be surrounded by a well material, then on that layer a barrier material can be grown, followed by another layer of self-assembled QDs, etc. This new structure is then essentially a multi-layered dots-in-a-well (DWELL) system. (see Fig. 4)

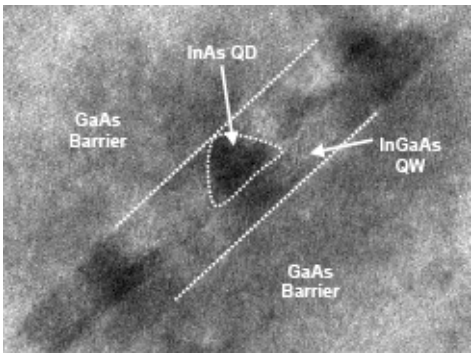

Figure 4: TEM image of quantum dots buried in a quantum well (image taken at the Center for High Technology Materials, University of New Mexico).

The array of self-organized InAs quantum dots are grown near the InAs/GaAs interface by using the strain effect at the interface. As a result, the electrons in the doped GaAs quantum well will sink into the ground state of the InAs QD, which has a much lower energy than the ground state of the quantum well. The deep potential well in the QD effectively reduces the dark current in this structure. When a photon is absorbed by electrons in the QDs, they will be excited to the ground state of the quantum well. For voltage-tunability, the photo-generated carriers in the quantum wells can be transported to the collector using the lateral transport scheme mentioned earlier. We can bury the quantum dots within one of a pair of undoped quantum wells and transport can be accomplished laterally, with the help of tunneling coupling between the wells (see Fig. 5). The key issue for operation in these QDIPs is to guarantee that the non-radiative transition lifetime of electrons in the quantum well ground state back to the QD ground state is longer than the tunneling time between the two quantum wells.

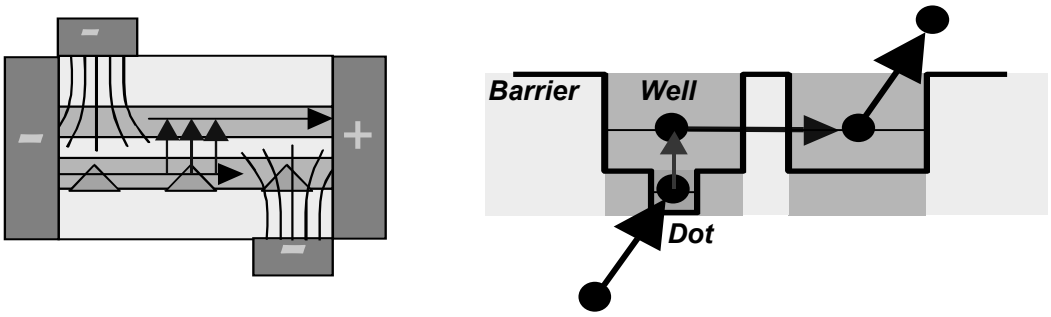

Figure 5: Laterally-biased double quantum well system, with quantum dots (triangles) embedded in the active well. On the left we see the conduction path from the source (-) to the drain (+), with top and bottom biasing gates. On the right is the bandstructure diagram for the transport process described in the text.

4. MAGNETIC TUNING

An idea that is a little further out in readiness level is the wavelength tuning of a QWIP's responsivity using a magnetic field. We have performed calculations using a self-consistent field theory including the Coulomb interaction between electrons that show when a magnetic field is applied parallel to the quantum well layer growth direction, there is the possibility of continuously tuning the QWIP response under a fixed bias voltage.[2] This tunability occurs when the magnetic Landau levels shift with the applied magnetic field strength (see Fig. 6).

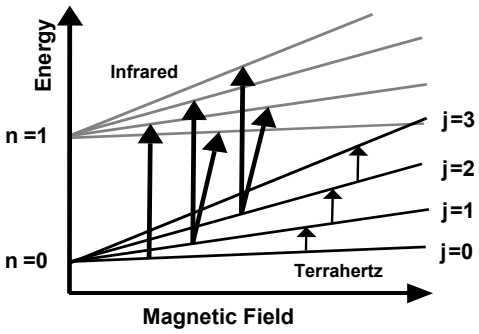

Figure 6: Calculations for a magnetic field parallel to the quantum well growth direction. The "n" states are quantum well electronic states; the "j" states are magnetic Landau states.

Bandgap engineering of semiconductor heterostructures can give rise to novel semiconductor quantum nanostructures that should respond to a normally-incident signal and have a tunable optical response in the presence of a magnetic field applied parallel to the growth direction. In one such nanostructure, very narrow quantum wells with only one confined electronic state each, are separated by barriers composed of a superlattice structure (separating layer thicknesses < 5 nm so that the electron wavefunctions overlap across the layers) with several minibands (see Fig. 7). When the parallel magnetic field is turned on, a ladder of Landau levels will be formed within the narrow well. By properly varying the magnitude of the magnetic field, the second Landau-level can be aligned with one of the minibands in the superlattice barrier. The inter-Landau-level transition inside the quantum well should respond to a normally-incident signal. The tuning of the peak wavelength could be accomplished by changing the magnitude of the magnetic field, which shifts the Landau-level within a single miniband or aligns the second Landau-level with different minibands.

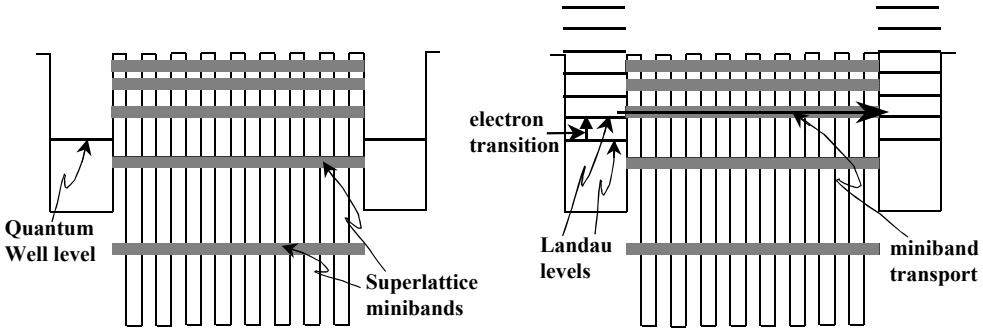

Figure 7: On the left is a possible structure for utilizing magnetic field tuning. Here, each quantum well has only a single discrete level and the superlattice barrier between the wells has several minibands. On the right, when a magnetic field is applied parallel to the growth direction of this structure, the single quantum well energy state splits into a ladder of Landau levels. If the magnetic field is tuned in strength, the j=2 Landau level can be made resonant with one of the minibands. A transition between j=1 and j=2 then will lead to miniband transport through the structure and a photocurrent can be measured.

5. POLARIZATION DETECTION WITHIN A SINGLE PIXEL

An imaging polarimeter captures an image with both the intensity and the average polarization state recorded for each pixel. A polarimetric image has more information than a simple intensity image and improves remote sensing and automatic target recognition. Polarimetry can be used to identify materials and to distinguish samples from a cluttered background. Polarimetry has also shown promise for mine detection, contrast enhancement, and shape determination. On average, polarimetric images of man-made objects have a higher degree of polarization than polarimetric images of natural objects. This pattern could be useful for spectro-polarimetric sub-pixel target detection.

All current polarimeters create multiple images with different polarizing filters. If the polarization is determined using simultaneous images on different focal planes, spatial resolution errors occur. If the polarization is determined using several consecutive images with a single focal plane, temporal registration errors will occur.

We have invented a scheme that should alleviate each of the errors mentioned above. In our device, shown in Fig. 8, quantum-well stacks are used in combination with linear gratings to determine the degree of polarization of incident light within a single pixel. The quantum well stacks do not absorb light having an electric field component in a plane parallel to the stacks (due to quantum mechanical selection rules in the quantum wells). The non-absorbed propagating light is reflected, diffracted, and transmitted at each grating as a function of its polarization. The z-polarized component of the light is absorbed by the quantum wells, thereby producing a photocurrent. The voltage bias across each quantum well stack is individually adjusted, and the photocurrent within each stack, which is proportional to the flux of light absorbed by that quantum-well stack, is read out separately. The circuit diagram for such a device is similar to that of existing multi-color QWIP devices. The four photocurrents can be linearly mapped to the four Stokes parameters that define the complete polarization vector of the incident light.

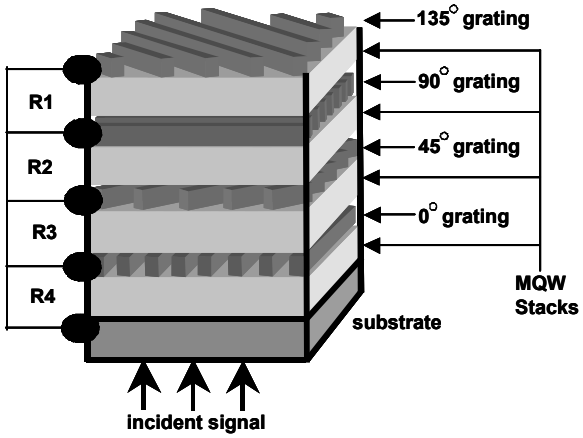

Figure 8: The polarimeter-in-a-pixel. A stack of multi-quantum-well photoconductors and gratings at different orientations. The photocurrent from each layer is read individually.

In order to validate the principle-of-operation described above, we developed a working electromagnetic model of the device using transfer-matrix techniques described.[3] Figure 9 shows the fraction of 9.5 micron incident light absorbed in the four quantum-well stacks versus the angle of linear polarization of the incident

light. These curves demonstrate that with the proper characterization of each polarimeter array, the relative photocurrents from the four quantum-well stacks should provide a means to measure the full polarization of incident light.

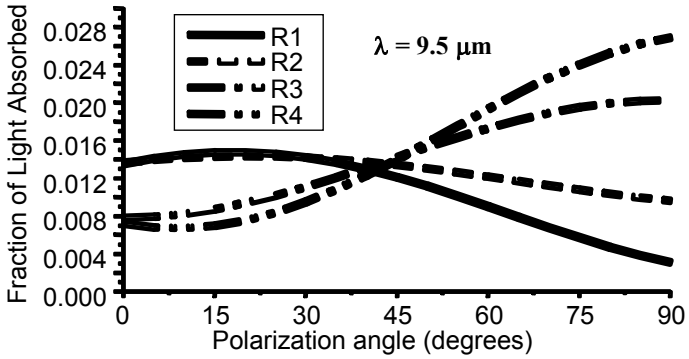

Figure 9: An example of the response from the four layers of the pixel-polarimeter as we rotate the polarization angle of the incident linearly-polarized light.

The next challenge was to find a process that would allow the fabrication of the device. We began with a proof-of-concept two-layer test structure. The purpose of this structure is to demonstrate the underlying physics of the proposed device, and to pave the way for fabricating the more complex four-layer structure. We used a wafer fusion approach to create the various layers of MQWs and gratings. For the two-layer device, the quantum wells were each grown on a perfect substrate and one set of gratings was etched on one wafer. A second wafer was then fused to the grating surface of the first wafer by Dr. Liau's group at the MIT Lincoln Laboratory, using a method they developed.[4] The top substrate was then removed and a second layer of gratings was etched on top. The final structure is shown in Fig. 10. This structure was then prepared for characterization, however there were some processing problems that need to be overcome first. The figure actually shows one of the problems we had. It shows a hole created when a contact was ripped off by accident.

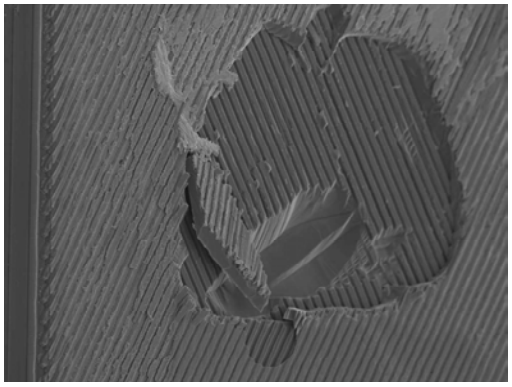

Figure 10: This is our first attempt at a proof-of-concept, two-grating-layer pixel polarimeter. The SEM picture shows a top layer of gratings, then a layer of quantum well material, then another layer of gratings, then another layer of quantum well material, followed finally by a substrate.

6. PHOTOLUMINESCENCE ("LASER") COOLING OF SOLIDS

Infrared photodetectors generally need to be cooled in order to work more efficiently. There are several approaches to cooling solid-state detectors, including mechanical cooling, thermoelectric cooling, thermionic cooling, opto-thermionic cooling, and fluorescent cooling. Some of these cooling concepts provide very attractive possibilities for cryogenics-on-a-chip, either including contacts for a current flow under a bias or excluding contacts by replacing the bias with a resonant optical field.

Solid state cooling will have many advantages for space-based sensing missions. Such a cooler will have no vibration to contend with. It should be free of electronic, magnetic, and electromagnetic noise. With no moving parts, it should have a very long lifetime. The solid-state cooling technologies are accomplished with low-cost materials and manufacturing, and should be highly reliable. A complete solid-state cryocooler with a cubic centimeter of volume (and in some cases, much less than that) seems possible. This extreme miniaturization could lead to cooling a focal plane array, pixel by pixel.

The cooling of a solid via light-induced fluorescence has been of interest for a very long time.[5] This interesting phenomenon involves the excitation of an electron from the valence bandedge to the conduction bandedge by absorbing a pump photon (see Fig. 11). This cool electron quickly becomes hot by gaining thermal energy through ultrafast electron-phonon scattering. After a radiative lifetime, recombination of the hot electron will produce a spontaneous photon with energy higher than that of the pump photon. As a result, the lattice will be cooled due to the loss of thermal energy to the electron. It is only recently that this phenomenon has been observed experimentally. Laser-induced fluorescent cooling of heavy-metal-fluoride glass doped with trivalent ytterbium ions was the first realization of this concept.[6] Soon to follow were demonstrations of cooling in dye solutions[7] and thulium-doped glass.[8]

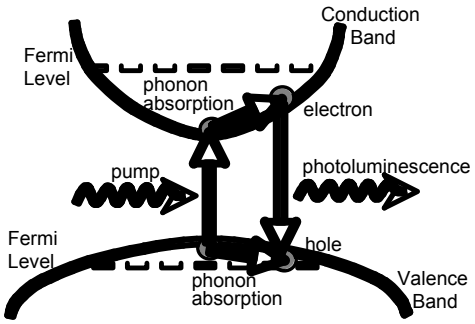

Figure 11: This is a band diagram of the photoluminescence cooling mechanism in semiconductors.

Laser cooling of a semiconductor remains an elusive goal, although it has been pursued for many years. The key question we have tried to answer is: what are the best semiconductor materials and conditions for achieving the greatest laser cooling effect? This requires an accurate *nonlocal* theory on a microscopic level, which directly provides an evolution equation for the lattice temperature by including the dynamical effects. We have developed such a *nonlocal* theory for the laser cooling of semiconductors.[9] By including the effect of the carrier distribution, we were able to uncover the essential physics underlying the phenomenon and we provided important quantitative predictions that can guide experimentalists toward achieving maximum efficiency of laser cooling in the future.

We assumed a weak pump laser first excites electrons from the valence bandedge to the conduction bandedge. The excited carriers instantaneously form a nonequilibrium distribution. It is well known that the quantum kinetics of the scattering of electrons with phonons or other carriers under a weak pump field can only be seen within the time scale of several hundred femtoseconds. Subsequently, ultrafast carrier-phonon and carrier-carrier scattering quickly adjusts the kinetic energies of these excited carriers by taking energy from the lattice. As a result, a quasi-equilibrium Fermi-Dirac distribution of carriers is formed in about 0.1 ps, with an electron temperature determined by the pump-field intensity, pump-photon energy, and lattice temperature. After a few tens of nanoseconds, radiative decay of the excited carriers will begin to affect the electron distribution. The electron temperature will be adiabatically readjusted according to an energy balance between the power-gain density due to optical absorption, the power-loss density due to photoluminescence, and the power-exchange density due to scattering with phonons. At the same time, the lattice temperature will evolve because of an imbalance between the power loss due to transferring phonon energy to carriers and the slight power gain from the external thermal radiation. Just before the radiative decay occurs, the lattice and the electrons are in thermal equilibrium with an initial temperature which can be determined by solving a semiconductor Bloch equation.

Using our nonlocal theory, we find that the laser-cooling rate is largest for a large bandgap material, a weaker pump-laser field, and a high initial lattice temperature (see Fig. 12). We also find that the laser-cooling power decreases as the lattice cools down.

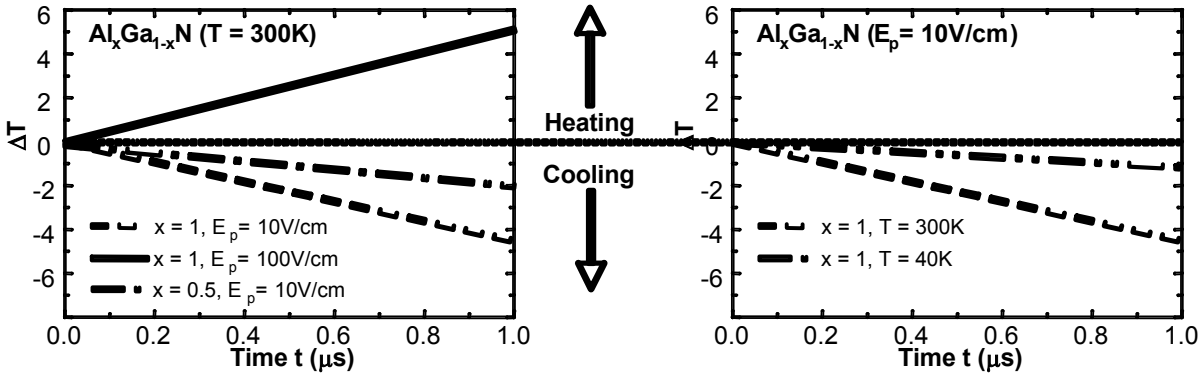

Figure 12: The graph on the left indicates that there is greater cooling for lower pump power and wider bandgap. The graph on the right indicates that there is greater cooling when the initial temperature is higher.

7. LASER COOLING OF SEMICONDUCTOR QUANTUM WELLS

We have generalized our above theory to a microscopic theory for spatially-selective laser cooling in undoped semiconductor quantum wells, which cools the part of the lattice inside the well region more than that outside the well in the barrier region.[10] Our model is based on the following four successive physical steps: (i) photo-excited cold carriers with nearly-zero kinetic energies are coherently and resonantly excited across a bandgap by a weak laser field; (ii) the photo-induced cold carriers in conduction and valence bands are heated to higher energy states above their chemical potentials via inelastic phonon scattering; (iii) the hot electrons and holes recombine through radiative decay giving rise to fluorescent photons, thus taking away more power from the quantum-well system than that acquired through the laser-field absorption; (iv) phonons in the system

thermally diffuse into the central cool region (quantum well) from two surrounding warm regions (barriers), thereby allowing the entire lattice to cool with time below the thermally-isolated surrounding environment. This model includes the transport of phonons due to the non-uniform spatial distribution of the lattice temperature. It also provides us with a time evolution of the profile of the lattice temperature through numerical calculations.

It has been known for a long time that the exciton effect at room temperature becomes negligible in GaAs quantum wells. However, the interaction between electron and hole plasmas is still expected to play a major role during the second step of the four-step laser cooling model. The resulting detailed balance between interacting electron and hole plasmas (due to carrier-carrier scattering) locks the carrier temperatures to a common value $T(z)$. The strong confinement of the photo-induced carriers within the quantum wells prevents carriers from diffusing in the z direction perpendicular to the quantum wells. Since the time for the carriers to adjust their temperature is much shorter than the evolution time of the lattice temperature, the conservation of total energy of confined electrons and holes gives rise to a detailed-energy-balance equation at each z position during the last step of the four-step model. This energy-balance equation can be used to adiabatically determine the spatial dependence of the carrier temperature $T(z)$ for each profile of the lattice temperature $T_L(z)$. The slow time evolution of the lattice-temperature profile $T_L(z)$ during the last step of the model is found to be determined by a thermal-diffusion equation for phonons. The carrier temperature will be thermally dragged down by the reduction of the lattice temperature with time.

At 300K, we predict a unique profile of the carrier temperature: a dip at z = 0 and a value lower than T_0 at the edge of sample (see left side of Fig. 13). This unique profile remains constant as the carrier temperature decreases down to around 40K. For this range of carrier temperatures, the inelastic phonon scattering of carriers is very effective and is dominated by longitudinal optical phonons. Although T_L becomes independent of z, T(z) still has a dip due to the lack of diffusion of carriers in the z direction. At 40K, the carrier temperature profile as a function of position T(z) becomes effectively suppressed while the carriers are cooled down and the feature disappears 6 μs after the start of photoluminescence (see right side of Fig. 13). This is due to the competition between thermal diffusion of acoustic phonons (both longitudinal and transverse) and carrier-phonon inelastic scattering.

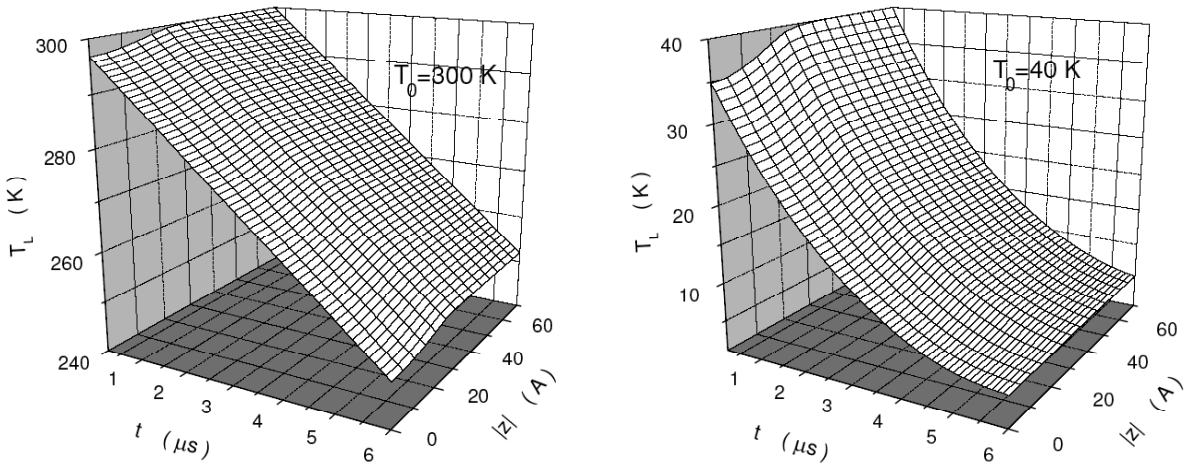

Figure 13: These are graphs of lattice temperature versus time and position. On the left we see the increase of the central dip at higher temperatures. On the right we see the flattening of the temperature profile at lower temperatures.

8. SUMMARY AND CONCLUSIONS

A wavelength-tuning capability in an IR sensor will provide the ability to successfully perform missions involving space-based intelligence and surveillance such as detection and identification of biological and chemical weapons storage and/or production facilities, and detection, identification, and tracking of tactical and strategic missiles during and after launch. Many space situational awareness missions will also be enabled by such a capability. If all of these various missions could be performed by a single, reconfigurable sensor system, the cost savings would be enormous. We have described several possible approaches to attaining this goal, all of which we are investigating in the Advanced Space-Based Detectors Research Group of the Space Vehicles Directorate, Air Force Research Laboratory. These approaches all utilize the discrete nature of electronic energy levels in quantum-confined structures, and the ability of external electric or magnetic fields to shift these levels around.

A polarization-detection capability will also provide additional information to any surveillance system. At the very least, it could provide the ability to queue higher resolution sensor systems when interesting polarization signatures are detected. We have described a new optoelectronic device that promises to detect, simultaneously and instantaneously, the four Stokes parameters that fully describe the polarization state of an ensemble of incident photons in a narrow wavelength band. Other techniques for capturing polarimetric images involve large errors at the edges of objects in the scene or require the designer to sacrifice spectral resolution or increase the weight by using beam splitters and multiple focal plane arrays. This new device uses the interference between multiple diffractions and reflections in a multi-layered structure of quantum wells and gratings to encode the polarimetric information in the multiple photocurrents that are read out from each layer. This device uses the ability of quantum wells to distinguish between polarizations parallel and perpendicular to the quantum well growth direction.

We have described a “new” (only in the sense of now it might be able to be accomplished) solid-state cooling scheme called laser or photoluminescent cooling. This cooling mechanism could lead to an extreme miniaturization of the cooling system, for on-chip, pixel-by-pixel cooling. This sort of cooling system is vibration and noise free, should be very reliable and robust, should have a long lifetime, and should be very low in cost.

Finally, we have described how this laser cooling scheme in quantum well heterostructures could be used to cool the carriers responsible for providing the photocurrent for detection purposes. The phonon-dragged carrier temperature is initially suppressed due to moderate LO phonon scattering at 77 K. It gradually increases with decreasing temperature due to weak TA and LA phonon scattering at lower temperatures. The carrier and lattice temperatures approach each other when the cooling stops. The initial temperature difference profile is seen to be larger in the barrier regions than in the well region. This is attributed to the suppression of the weak exchange of thermal energy between carriers and phonons in the barrier region due to the lack of carriers there. This could lead to improved ways to cool quantum well infrared photodetectors for space applications.

REFERENCES

1 S. Ragavan, P. Rotella, A. Stinz, B. Fuchs, S. Krishna, C. Morath, D. A. Cardimona, and S. W. Kennerly, Appl. Phys. Lett. **81**, 1369 (2002).
2 D. Huang and S. K. Lyo, J. Appl. Phys. **83**, 4531 (1998); *ibid*, Phys. Rev. B **59**, 7600 (1999).
3 M. Serna, Inf. Phys. & Tech. **44**, 457 (2003).
4 Z. L. Liau and D. E. Mull, Appl. Phys. Lett. **56**, 737 (1990).
5 P. Pringsheim, Z. Phys. **57**, 739 (1929).
6 R. I. Epstein, M. I. Buchwald, B. C. Edwards, T. R. Gosnell, and C. E. Mungan, Nature (London) **37**, 500 (1995).
7 J. L. Clark and G. Rumbles, Phys. Rev. Lett. **76**, 2037 (1996).
8 C. W. Hoyt, M. Sheik-Bahae, R. I. Epstein, B. C. Edwards, and J.E. Anderson, Phys. Rev. Lett. **85**, 3600 (2000).
9 D. H. Huang, T. Apostolova, P. M. Alsing, and D. A. Cardimona, Phys. Rev. B **70**, 033203 (2004).
10 D. H. Huang, T. Apostolova, P. M. Alsing, and D. A. Cardimona, to be published in Infr. Phys. & Tech. (2005).